Journal of Southeast University (English Edition) Vol. 28, No. 1, pp. 79 - 84 Mar. 2012 ISSN 1003—7985

Constitutive model for concrete subjected to impact loading

Liu Haifeng[1] Ning Jianguo[2]

([1]Department of Civil and Hydraulic Engineering, Ningxia University, Yinchuan 750021, China)

([2]State Key Laboratory of Explosion Science and Technology, Beijing Institute of Technology, Beijing 100081, China)

Abstract: To better design and analyze concrete structures, the mechanical properties of concrete subjected to impact loadings are investigated. Concrete is considered to be a two-phase composite made up of micro-cracks and solid parts which consist of coarse aggregate particles and a cement mortar matrix. The cement mortar matrix is assumed to be elastic, homogeneous and isotropic. Based on the Mori-Tanaka concept of average stress and the Eshelby equivalent inclusion theory, a dynamic constitutive model is developed to simulate the impact responses of concrete. The impact compression experiments of concrete and cement mortar are also carried out. Experimental results show that concrete and cement mortar are rate-dependent. Under the same impact velocity, the load-carrying capacity of concrete is higher than that of cement mortar. Whereas, the maximum strain of concrete is lower than that of cement mortar. Regardless of whether it is concrete or cement mortar, with the increase in the impact velocity, the fragment size of specimens after experiment decreases.

Key words: concrete; micromechanics; dynamic constitutive model; impact loading

doi: 10.3969/j.issn.1003-7985.2012.01.014

As one of the main structure and engineering materials, concrete has been widely used in civil and industrial construction. The structures may be subjected to normal loads such as weight, and they are also exposed to impact loadings due to explosions and earthquakes. To better design and analyze these structures, it is necessary to investigate the mechanical characteristics of concrete subjected to impact loadings.

There is much literature on the rate sensitivity of concrete[1-4]. The early tests on concrete under dynamic loading are performed with pendulum and drop weight tests. The split Hopkinson pressure bar (SHPB) and the one-stage light gas gun apparatus are also used to study the dynamic mechanical properties of concrete. According to the experiments above, concrete is rate-dependent.

Currently, there are many kinds of dynamic constitutive models for concrete [5-7]. The common characteristic of those models is that they have too many parameters, some of which are very difficult to be determined by experiments. However, there are few documents on the dynamic constitutive model for concrete from a micromechanical viewpoint.

In this paper, concrete is considered to be a two-phase composite made up of micro-cracks and solid parts which consist of coarse aggregate particles and a cement mortar matrix. Suppose that the cement mortar matrix is elastic, homogeneous and isotropic. On the basis of the Mori-Tanaka average stress concept and the Eshelby equivalent inclusion theory, a dynamic constitutive model for concrete is established. At the same time, the impact compression experiment and the quasi-static experiment on concrete and cement mortar are carried out.

1 Constitutive Relation

Concrete typically consists of micro-cracks and solid parts which contains coarse aggregate particles and a cement mortar matrix. Assume that the strain is small and the concrete strain $\boldsymbol{\varepsilon}$ is the composition of elastic strain $\boldsymbol{\varepsilon}^{\mathrm{e}}$ and nonlinear strain $\boldsymbol{\varepsilon}^{\mathrm{d}}$,

$$\boldsymbol{\varepsilon} = \boldsymbol{\varepsilon}^{\mathrm{e}} + \boldsymbol{\varepsilon}^{\mathrm{d}} \tag{1}$$

where $\boldsymbol{\varepsilon}^{\mathrm{e}}$ is the strain associated with the solid prior to damage accumulation; $\boldsymbol{\varepsilon}^{\mathrm{d}}$ is the strain due to the presence of initial micro-cracks and the subsequent growth of tensile micro-cracks.

Based on the Hook law, the elastic relationship is also assumed to be between the elastic strain $\boldsymbol{\varepsilon}^{\mathrm{e}}$ and the stress $\boldsymbol{\sigma}$,

$$\boldsymbol{\varepsilon}^{\mathrm{e}} = \boldsymbol{M} : \boldsymbol{\sigma} \tag{2}$$

where $\boldsymbol{M}$ is the compliance tensor of the solid,

$$\boldsymbol{M} = \frac{(c_1+1)(1+\nu)}{4E}\begin{bmatrix} 1 & \dfrac{c_1-3}{c_1+1} \\ \dfrac{c_1-3}{c_1+1} & 1 \end{bmatrix}$$

For the plane stress, $c_1 = (3-\nu)/(1+\nu)$; for the plane strain, $c_1 = (3-4\nu)$; E and ν are Young's modulus and Poisson's ratio of the solid.

Received 2011-11-01.

Biography: Liu Haifeng(1975—), male, doctor, liuhaifeng1557@163.com.

Foundation items: The National Natural Science Foundation of China (No. 11162015), the Natural Science Foundation of Ningxia Hui Autonomous Region (No. NZ1106).

Citation: Liu Haifeng, Ning Jianguo. Constitutive model for concrete subjected to impact loading[J]. Journal of Southeast University (English Edition), 2012, 28(1): 79 - 84. [doi: 10.3969/j.issn.1003-7985.2012.01.014]

1.1 Elastic constants of solid

As mentioned above, the solid part is regarded to be a two-phase composite consisting of coarse aggregate particles and the cement mortar matrix. The volumetric modulus of the coarse aggregate particles and the cement mortar matrix are denoted by k and k_0, respectively, and their shear moduli are denoted by μ_1 and μ_0. Let f_1 and f_0 be the volume fractional concentrations of the coarse aggregate particles and the cement mortar matrix, respectively. Based on the concept of average stress by Mori and Tanaka[8] and the Eshelby equivalent inclusion theory[9], the overall volumetric modulus k and shear modulus μ of the solid are defined as

$$\left.\begin{aligned} \frac{k}{k_0} &= 1 + \frac{f_1}{\dfrac{3f_0k_0}{3k_0+4\mu_0} + \dfrac{k_0}{k_1-k_0}} \\ \frac{\mu}{\mu_0} &= 1 + \frac{f_1}{\dfrac{6}{5}\dfrac{f_0(k_0+2\mu_0)}{3k_0+4\mu_0} + \dfrac{\mu_0}{\mu_1-\mu_0}} \end{aligned}\right\} \tag{3}$$

Based on the elastic theory, the Young modulus E and the Poisson ratio ν of the solid are

$$E = \frac{9k\mu}{3k+\mu}, \quad \nu = \frac{3k-2\mu}{6k+2\mu} \tag{4}$$

1.2 Nonlinear strain

On the basis of the sliding crack model for brittle material[10–14], the new micro-cracks in cement mortar are nucleated approximately along the maximum principal compressive stress. The new micro-cracks and pre-existing micro-cracks along the maximum principal compressive stress grow and interact with each other, thus forming macro-cracks and finally leading to the fracture of the cement mortar.

For concrete, there are many micro-cracks of random sizes and orientations.

All the initial micro-cracks are assumed to be located on the interface between the cement mortar and the aggregate facet (see Fig. 1(a)). With the increase in applied external compressive load, the growth of kinking cracks will be initiated. When the stress intensity factor K_I of the wing crack reaches the fracture toughness K_{IC}, the wing crack grows along a curved path and eventually turns parallel to the applied stress (see Figs. 1(b) and c).

For simplicity, suppose that these micro-cracks are of the same size, distributed homogeneously and parallel to each other. The nonlinear strain caused by micro-crack growth is

$$\boldsymbol{\varepsilon}^{\mathrm{d}} = N\begin{bmatrix} \Delta\varepsilon_1 \\ \Delta\varepsilon_2 \end{bmatrix} \tag{5}$$

where $\Delta\varepsilon_1$ and $\Delta\varepsilon_2$ are the strain due to individual micro-cracks along the coordinate system direction, and N is the micro-crack density.

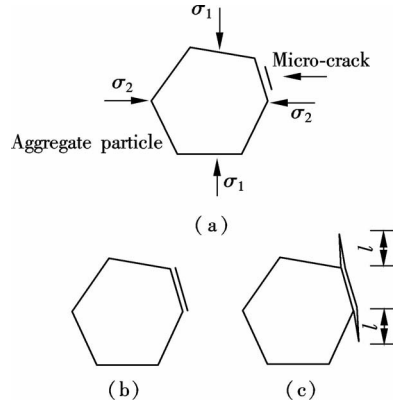

Fig. 1 Growth of individual micro-crack. (a) Initial state; (b) Growth of crack; (c) Kinking of the crack

The linear relationship between the strain $\Delta\varepsilon_1$, $\Delta\varepsilon_2$ and the stress σ_1 and σ_2 is assumed. Based on the sliding crack model of brittle material subjected to biaxial compressive stress [10–14], $\Delta\varepsilon_1$ and $\Delta\varepsilon_2$ are expressed as

$$\begin{bmatrix} \Delta\varepsilon_1 \\ \Delta\varepsilon_2 \end{bmatrix} = \begin{bmatrix} S_{11} & S_{12} \\ S_{21} & S_{22} \end{bmatrix}\begin{bmatrix} \sigma_1 \\ \sigma_2 \end{bmatrix} \tag{6}$$

where S_{ij} are constants, which can be expressed in the following forms by the coefficient comparison.

$$\left.\begin{aligned} S_{11} &= \frac{A_1B_1 + A_2B_2}{E} = \frac{1}{E}\left[A_1\ln\left(1+\frac{l}{l_*}\right) + A_2\sqrt{\frac{l+l_{**}}{l+l_*}}\right] \\ S_{22} &= \frac{A_3B_1 + C_1 + A_4B_3 - A_5B_2 - A_6B_4}{E} \\ S_{12} &= S_{21} = \frac{A_7B_1 + A_8B_3 + A_9B_2 + A_{10}B_4}{E} \end{aligned}\right\} \tag{7}$$

where $A_i (i = 1, 2, \ldots, 10)$ and C_1 are parameters related to size $2c$ and the orientation angel θ of a primitive micro-cracks; $B_i (i = 1, 2, 3, 4)$ are parameters connected with tensile wing micro-cracks; l_* and l_{**} are equal to $0.27c$ and $0.083c$, respectively[14].

Then the overall strain is

$$\begin{bmatrix} \varepsilon_1 \\ \varepsilon_2 \end{bmatrix} = \begin{bmatrix} \varepsilon_1^{\mathrm{e}} + \varepsilon_1^{\mathrm{d}} \\ \varepsilon_2^{\mathrm{e}} + \varepsilon_2^{\mathrm{d}} \end{bmatrix} = \frac{(c_1+1)(1+\nu)}{4E}\begin{bmatrix} 1 & \dfrac{c_1-3}{c_1+1} \\ \dfrac{c_1-3}{c_1+1} & 1 \end{bmatrix}\cdot \begin{bmatrix} \sigma_1 \\ \sigma_2 \end{bmatrix} + N\begin{bmatrix} S_{11} & S_{12} \\ S_{21} & S_{22} \end{bmatrix}\begin{bmatrix} \sigma_1 \\ \sigma_2 \end{bmatrix} \tag{8}$$

Under the one-dimensional stress ($\sigma_2 = 0$), the relationship between the stress and the strain is

$$\varepsilon_1 = \frac{\sigma_1}{E} + NS_{11}\sigma_1, \quad \varepsilon_2 = -\nu\frac{\sigma_1}{E} + NS_{12}\sigma_1 \tag{9}$$

Substituting σ_1 and ε_1 in Eq. (9) with σ and ε, respectively, we obtain

$$\sigma = \frac{E}{\left[1 + NA_1 \ln\left(1 + \frac{l}{l_*}\right) + NA_2 \sqrt{\frac{l + l_{**}}{l + l_*}}\right]} \varepsilon \quad (10)$$

Eq. (10) can be written in a simple form,

$$\sigma = \bar{E}\varepsilon$$

where $\bar{E}$ is the effective elastic modulus.

Parameter D is introduced to denote the attenuation effect of the micro-crack density and the growth of the micro-crack on the elastic modulus. Then,

$$\bar{E} = (1 - D)E \quad (11)$$

where

$$D(N, l) = \frac{NA_1 \ln\left(1 + \frac{l}{l_*}\right) + NA_2 \sqrt{\frac{l + l_{**}}{l + l_*}}}{1 + NA_1 \ln\left(1 + \frac{l}{l_*}\right) + NA_2 \sqrt{\frac{l + l_{**}}{l + l_*}}} \quad (12)$$

2 Description of Micro-Crack Damage

2.1 Micro-crack growth criteria

Concrete is rate-dependent. When subjected to impact loading, the micro-crack growth criteria is

$$K_I \geqslant K_{Id}(\dot{l}) \quad (13)$$

where $K_{Id}(\dot{l})$ is the fracture toughness of concrete subjected to impact loading. After the theoretical analyses and experimental researches, Freund and Hutchinson[15] proposed the following equation of fracture toughness under the action of impact loading,

$$K_{Id}(\dot{l}) = \frac{K_{IC}}{(1 - \dot{l}/C_R)^{\beta}} \quad (14)$$

where K_{IC} is the initial value of fracture toughness under the quasi-static conditions; β is the experimental fit coefficient; $\dot{l}$ is the growth rate of the micro-crack; C_R is the Rayleigh wave velocity, which is determined by

$$C_R = \frac{0.862 + 1.14\nu}{1 + \nu} \sqrt{\frac{E}{2(1 + \nu)\rho}}$$

where ρ is the concrete density and ν is the Poisson ratio.

2.2 Micro-crack nucleation

The micro-crack nucleation is a random process. Grady and Kipp[16] presented a micro-crack damage model when researching on the explosion of shale. In the model, the micro-crack density N and the strain ε satisfy the two-parameter Weibull distribution,

$$N = k_2 \varepsilon^m \quad (15)$$

where k_2 and m are the parameters to describe the fracture behavior of the material.

2.3 Micro-crack growth

When researching on micro-cracks, Wang[17] found that the growth of micro-cracks is connected with the dimensions of the micro-cracks and the current stress state. Based on the energy balance, a growth model of the micro-crack is given in the following form,

$$\frac{\dot{l}}{l} = \frac{1 - \nu^2}{2\lambda_1 E} \pi (\sigma_t^2 - \sigma_{th}^2) C_R \quad (16)$$

where λ_1 is the specific surface energy per area; σ_t is the interior tensile stress caused by the damage evolution of micro-cracks, which is usually not equal to the value of the exterior stress σ_{ij}. For the sake of simplicity, the interior tensile stress σ_t is given by

$$\sigma_t = \beta_1 \sqrt{\frac{3}{2} s_{ij} s_{ij}} \quad (17)$$

where β_1 is the material coefficient and s_{ij} ($= \sigma_{ij} - 1/3\sigma_{ii}$) is the deviatoric stress tensor.

According to the critical conditions for brittleness fracture caused by the Irwin micro-crack instability[18], the threshold stress for micro-crack nucleation can be expressed as

$$\sigma_{th} = \frac{K_{IC}}{f\left(\frac{c}{W}\right) \sqrt{\pi a_{th}}} \quad (18)$$

where a_{th} is the critical nucleation size whose value depends on the material properties. $f\left(\frac{c}{W}\right)$ is a function dependent on the geometrical size of the concrete specimen, given in the following form,

$$\begin{aligned} f\left(\frac{c}{W}\right) = \left(1 - \frac{c}{W}\right)^{-3/2} \Big[& 1.121\,4 + 0.029\,4 \frac{c}{W} - \\ & 2.190\,7\left(\frac{c}{W}\right)^2 + 3.551\,1\left(\frac{c}{W}\right)^3 - \\ & 6.245\,9\left(\frac{c}{W}\right)^4 - 21.185\,3\left(\frac{c}{W}\right)^5 + \\ & 20.046\,3\left(\frac{c}{W}\right)^6 - 6.496\,7\left(\frac{c}{W}\right)^7 \Big] \end{aligned} \quad (19)$$

where W is the transverse size of the specimen. Because the value of $f\left(\frac{c}{W}\right)$ is near to 1.0, for simplicity, let $f\left(\frac{c}{W}\right) = 1.0$ in the model.

3 One-Dimensional Dynamic Constitutive Model

A one-dimensional dynamic constitutive model for concrete is

$$\left.\begin{aligned} \dot{\sigma} &= E\dot{\varepsilon} && \varepsilon < \varepsilon_{th} \\ \dot{\sigma} &= E\dot{\varepsilon} - E(\dot{D}\varepsilon + D\dot{\varepsilon}) && \varepsilon \geqslant \varepsilon_{th} \end{aligned}\right\} \quad (20)$$

where the range of ε_{th} is from one fourth to one fifth of the peak strain.

Damage D is defined by Eq. (12). The evolution equation of the damage is

$$D = \frac{k_2 m \varepsilon^{m-1} \dot{\varepsilon} \left[A_1 \ln\left(1 + \frac{l}{l_*}\right) + A_2 \sqrt{\frac{l + l_{**}}{l + l_*}} \right]}{\left[1 + k_2 A_1 \varepsilon^m \ln\left(1 + \frac{l}{l_*}\right) + k_2 A_2 \varepsilon^m \sqrt{\frac{l + l_{**}}{l + l_*}} \right]^2} + \frac{k_2 \varepsilon^m \dot{l} \left[\frac{A_1}{l + l_*} + \frac{A_2}{2} \left(\frac{l + l_{**}}{l + l_*} \right)^{-1/2} \frac{(l_* - l_{**})^2}{l + l_*} \right]}{\left[1 + k_2 A_1 \varepsilon^m \ln\left(1 + \frac{l}{l_*}\right) + k_2 A_2 \varepsilon^m \sqrt{\frac{l + l_{**}}{l + l_*}} \right]^2} \quad (21)$$

According to the elastic theory, the elastic modulus, the Poisson ratio, the volume modulus and the shear modulus meet the following relationships,

$$k_i = \frac{E_i}{3(1 - 2\nu_i)}, \quad \mu_i = \frac{E_i}{2(1 + \nu_i)} \qquad i = 0, 1 \quad (22)$$

where subscript $i = 0$ is consistent with the cement mortar matrix, and $i = 1$ with the coarse aggregate particles.

By combining Eq. (22) with material parameters obtained from the quasi-static experiment, the volume modulus and the shear modulus of the cement mortar matrix and the coarse aggregate particles are obtained. From Eq. (3) and Eq. (4), the elastic modulus, the Poisson ratio, the volume modulus and the shear modulus of the concrete can be obtained.

4.2 Experimental analysis

In the test, there are four groups of experiments with different strain rates in each. To simplify the analysis, the values of the strain rates are averaged. Therefore, the strain rate can be considered to be a constant in the test. Fig. 2 shows the comparison between the stress-strain curves of concrete and those of cement mortar. With the same strain rate, the load-carrying capacity of concrete is higher than that of cement mortar due to the influences of the coarse aggregate particles. However, the maximum strain of concrete is lower than that of cement mortar.

It can also be seen from Fig. 2 that the load-carrying capacities of concrete and cement mortar increase correspondingly with the strain rate. So concrete and cement mortar are rate-dependent.

The comparison of the experimental results with the simulated results from the constitutive model is shown in Fig. 3, where σ_d is the dynamic compressive strength and σ_s is the quasi-static compressive strength. The model parameters are as follows: The fracture toughness K_{IC} = 0.09 MPa · $m^{1/2}$; the surface energy $\lambda_1 = 0.08$ MJ · m^{-2};

4 Model Parameters

4.1 Experiment

A 74-mm-diameter split Hopkinson pressure bar (SHPB) is used to test concrete specimens. The mix proportions of concrete are listed in Tab. 1. For comparison purposes, cement mortar specimens are also made. The cement mortar has the same composition as the mortar phase in the concrete. The specimens were wet-cured for seven days, then stored in the laboratory until testing. During the period of air-drying, the ends of the specimens were ground plane and parallel with each other.

Tab. 1 Composition of concrete specimens

Ingredient	Cement	Coal ash	Silicon ash	Sand	Aggregate particles	Water	HSG	AE
Mass/g	300	50	20	300	500	125	2.5	2.5

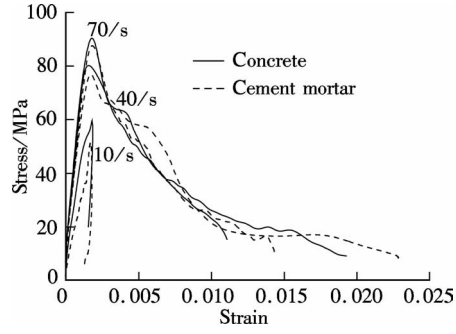

Fig. 2 The stress-strain curves of concrete and cement mortar at different strain rates

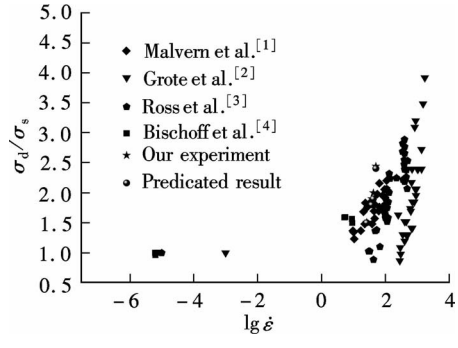

Fig. 3 Comparison of the predicated results and the experimental results

the material coefficient $\beta_1 = 0.2$; the nucleation parameter $k_2 = 3 \times 10^{20}$; $m = 6$; the critical nucleation size $a_{th} = 0.001$; the size of micro-crack $2c = 60$ μm; the orientation of micro-crack $\theta = 45°$; and the fit parameter $\beta = 1$.

Some typical pictures of the concrete and cement mortar specimens after the experiments are shown in Fig. 4 and Fig. 5, from which we can find that:

1) Regardless of whether it is concrete or cement mortar, with the increase in the impact velocity, the size of the specimen after the experiments decreases. When the

specimens are at a low strain rate, a few micro-cracks grow stably and unite, then expand unstably and lead to bigger pieces. However, when specimens are at a high strain rate, a large amount of micro-cracks grow and unite simultaneously, and then make the specimens fragment into smaller pieces.

2) As we know, there are many coarse aggregate particles in the concrete. Micro-cracks may be nucleated on the interface between the coarse aggregate particles and the cement mortar. With the same impact velocity, there are more micro-cracks to grow and interact with each other in the concrete specimens than in the cement mortar specimens. So the fragments of the concrete specimens are smaller than those of the cement mortar specimens.

3) The concrete and cement mortar specimens after the experiments become quadrilateral cones in the quasi-static compression experiment. Whereas, the concrete and cement mortar specimens after the tests keep intact with a strain rate of 10/s. When the strain rate is equal to 10/s, the duration time of impact loading is so short that there is not enough energy for pre-existing micro-cracks to grow and new micro-cracks to be nucleated. The specimens after the tests keep intact. While in the quasi-static compression experiment, though the strain rate is very low, the duration time of loading is so long that there is enough energy for pre-existing micro-cracks to grow and new micro-cracks to be nucleated. So the specimens after the experiments become quadrilateral cones.

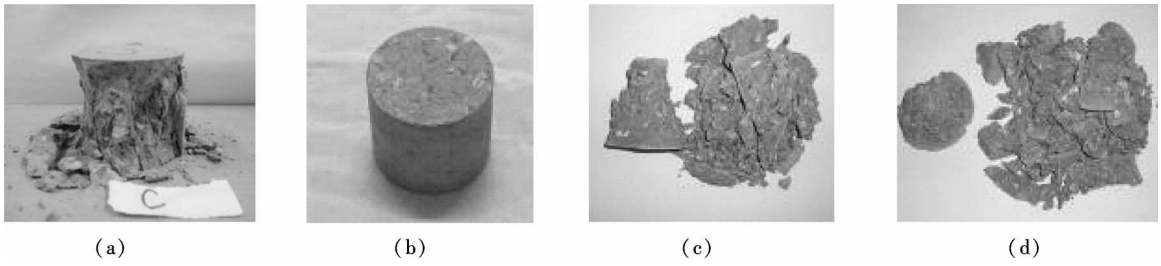

Fig. 4 Typical fragment photo of concrete. (a) $\dot{\varepsilon}=1.2\times10^{-5}$/s; (b) $\dot{\varepsilon}=10$/s; (c) $\dot{\varepsilon}=40$/s; (d) $\dot{\varepsilon}=70$/s

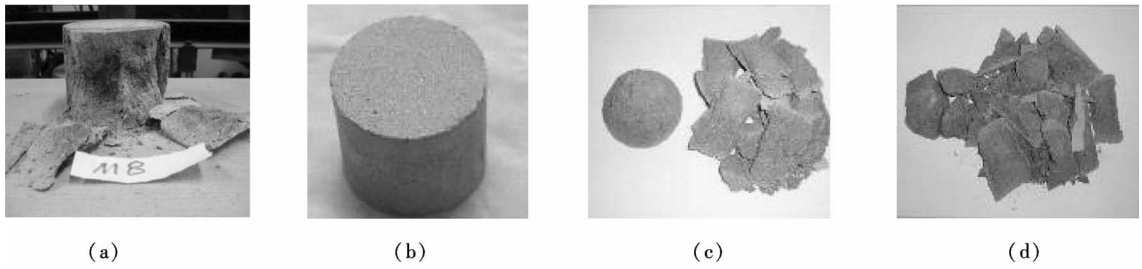

Fig. 5 Typical fragment photo of cement mortar. (a) $\dot{\varepsilon}=1.2\times10^{-5}$/s; (b) $\dot{\varepsilon}=10$/s; (c) $\dot{\varepsilon}=40$/s; (d) $\dot{\varepsilon}=70$/s

5 Conclusion

In this paper, concrete is considered to be a two-phase composite made up of micro-cracks and a solid part which consists of coarse aggregate particles and a cement mortar matrix. On the basis of the Mori-Tanaka concept of average stress and the Eshelby equivalent inclusion theory, a dynamic constitutive model is established to simulate the impact responses of concrete. The impact compression experiments on concrete and cement mortar are also carried out. Experimental results show that concrete and cement mortar are rate-dependent. The load-carrying capacity of concrete is higher than that of cement mortar. Regardless of whether it is concrete or cement mortar, with the increase in the impact velocity, the fragment size of specimens after the experiments decreases.

References

[1] Malvern L E, Jenkins D A, Tang T X, et al. Dynamic compressive testing of concrete [C]// *Proceedings of Second Symposium on the Interaction of Non-Nuclear Munitions with Structures.* Panama City Beach, FL, USA, 1984:194 - 199.

[2] Grote D L, Park S W, Zhou M. Dynamic behavior of concrete at high strain rates and pressures: experimental characterization [J]. *International Journal of Impact Engineering*, 2001, **25**(9):869 - 886.

[3] Ross C A, Tedesco J W, Kuennen S T. Effects of strain rate on concrete strength [J]. *ACI Materials Journal*, 1995, **92**(1):37 - 47.

[4] Bischoff P H, Perry S H. Impact behavior of plain concrete in uniaxial compression[J]. *Journal of Engineering Mechanics*, 1995, **121**(6):685 - 693.

[5] Ning J G, Shang L, Sun Y X. Investigation on impact behavior of concrete[J]. *Acta Mechanica Sinica*, 2006, **38**(2):199 - 208.

[6] Bhatti A Q, Kishi N. Constitutive model for absorbing system of RC girders used in rock-sheds under falling weight impact loading test[J]. *Journal of Nuclear Engineering and Design*, 2010, **240**(10):2626 - 2632.

[7] Georgin J F, Reynouard J M. Modeling of structures subjected to impact: concrete behavior under high strain rate [J]. *Cement and Concrete Composites*, 2003, **25**(1): 131 - 143.
[8] Morit T, Tanaka K. Average stress in matrix and average energy of materials with misfitting inclusions[J]. *Acta Metallurgica et Materialia*, 1973, **21**(5):571 - 574.
[9] Eshelby J D. The Determination of the elastic field of an ellipsoidal inclusion and related problems[J]. *Proceedings of the Royal Society A*, 1957, **241**(1226): 376 - 396.
[10] Ravichandran G, Subhash G. A micromechanical model for high strain rate behavior of ceramics[J]. *International Journal of Solids and Structures*, 1995, **32**(17/18): 2627 - 2646.
[11] Deng H, Nemat-Nasser S. Dynamic damage evolution in brittle microcracking solids[J]. *Mechanics of Materials*, 1992, **14**(2):83 - 103.
[12] Nemat-Nasser S, Obata N. A microcrack model of dilatancy in brittle materials[J]. *Journal of Applied Mechanics*, 1988, **55**(2):24 - 35.
[13] Huang C Y, Subhash C, Vitton S J. A dynamic damage growth model for uniaxial compressive response of rock aggregates[J]. *Mechanics of Materials*, 2002, **34**(5): 267 - 277.
[14] Horii H, Nemat-Nasser S. Elastic fields of interaction inhomogeneities[J]. *International Journal of Solids and Structures*, 1985, **21**(7):731 - 745.
[15] Freund L B, Hutchinson J W. High strain-rate crack growth in rate-dependent plastic solids[J]. *Journal of the Mechanics and Physics of Solids*, 1985, **33**(2): 169 - 191.
[16] Grady D E, Kipp M E. Continuum modeling of explosive fracture in oil shale[J]. *International Journal of Rock Mechanics and Mining Science*, 1980, **17**(1):147 - 157.
[17] Wang D R. Research on numerical simulation and engineering analysis methods of penetration phenomenon at high speed[D]. Hefei: Department of Mechanics of University of Science and Technology of China, 2002:44 - 46. (in Chinese)
[18] Wang D. *Fracture mechanics*[M]. Harbin: Harbin Institute of Technology Press, 1989:16 - 18. (in Chinese)

冲击载荷作用下混凝土本构模型

刘海峰[1] 宁建国[2]

([1] 宁夏大学土木与水利工程学院,银川 750021)
([2] 北京理工大学爆炸科学与技术国家重点实验室,北京 100081)

摘要:为了更好地设计和分析混凝土结构,对冲击荷载作用下混凝土材料的力学特性进行了研究. 将混凝土材料看成实体和微裂纹组成的复合材料,其中实体由粗骨料和水泥砂浆基体组成. 假设水泥砂浆基体为弹性的、均匀的和各向同性的. 基于 Mori-Tanaka 理论和 Eshelby 等效夹杂理论建立了冲击荷载作用下混凝土材料的动态本构模型. 同时,进行了混凝土和水泥砂浆的冲击压缩试验. 实验表明:混凝土和水泥砂浆都是率相关材料. 在相同的冲击速度下,混凝土比水泥砂浆具有更高的承载能力,但混凝土的最大应变低于水泥砂浆材料. 不论混凝土材料还是水泥砂浆材料,随着冲击速度的提高,破坏实验后试件的尺寸都逐渐减小.

关键词:混凝土;细观力学;动态本构模型;冲击荷载
中图分类号:O347